Hydrol. Earth Syst. Sci. Discuss., doi:10.5194/hess-2016-92, 2016
Manuscript under review for journal Hydrol. Earth Syst. Sci.
Published: 2 March 2016

Hydrology and Earth System Sciences
Open Access
Discussions

Incorporation of globally available datasets into the cosmic-ray neutron probe method for estimating field scale soil water content

William Alexander Avery[1], Catherine Finkenbiner[1], Trenton E. Franz[1], Tiejun Wang[1], Anthony L. Nguy-Robertson[1], Andrew Suyker[1], Timothy Arkebauer[1,2], and Francisco Munoz-Arriola[1,3]

[1]School of Natural Resources, University of Nebraska-Lincoln

[2]Department of Agronomy and Horticulture, University of Nebraska-Lincoln

[3]Biological Systems Engineering, University of Nebraska-Lincoln

Keywords: Cosmic-ray neutron probe; soil moisture; calibration parameters; remote sensing; maize; soybean

Corresponding author T.E. Franz (tfranz2@unl.edu)

Abstract

The need for accurate, real-time, reliable, and multi-scale soil water content (*SWC*) monitoring is critical for a multitude of scientific disciplines trying to understand and predict the earth's terrestrial energy, water, and nutrient cycles. One promising technique to help meet this demand is fixed and roving cosmic-ray neutron probes (CRNP). However, the relationship between observed low-energy neutrons and *SWC* is affected by local soil and vegetation calibration parameters. This effect may be accounted for by a calibration equation based on local

Hydrol. Earth Syst. Sci. Discuss., doi:10.5194/hess-2016-92, 2016
Manuscript under review for journal Hydrol. Earth Syst. Sci.
Published: 2 March 2016

Hydrology and Earth System Sciences
Discussions

soil type and the amount of standing biomass. However, determining the calibration parameters for this equation is labor and time intensive, thus limiting the full potential of the roving CRNP in large surveys and long transects, or its use in novel environments. In this work, our objective is to develop and test the accuracy of using globally available datasets (clay weight percent, soil bulk density, and soil organic carbon) to support the operability of the CRNP. Here, we develop a 1 km product of soil lattice water over the CONtinental United States (CONUS) using a database of *in-situ* calibration samples and globally available soil taxonomy and soil texture data. We then test the accuracy of the global dataset in the CONUS using comparisons from 61 *in-situ* samples of clay percent (RMSE = 5.45 wt. %, R^2 = 0.68), soil bulk density (RMSE = 0.173 g/cm^3, R^2 = 0.203), and soil organic carbon (RMSE = 1.47 wt. %, R^2 = 0.175). Next, we conduct an uncertainty analysis of the global soil calibration parameters using a Monte Carlo error propagation analysis (maximum RSME ~0.035 cm^3/cm^3 at a *SWC* = 0.40 cm^3/cm^3). In terms of vegetation, fast growing crops (i.e. maize and soybeans) contribute to the CRNP signal primarily through the water within their biomass and this signal must be minimized for accurate estimation of *SWC*. We estimated the biomass water signal by using a vegetation index derived from MODIS imagery as a proxy for standing wet biomass (RMSE < 1 kg/m^2). Lastly, we make recommendations on the design and validation of future roving CRNP experiments.

1. Introduction

By the year 2050, over nine billion people are predicted to inhabit the Earth (United Nations, 2015). The monumental task of feeding the projected global population will require a near doubling of grain production (FAO, 2009). As of today, the majority (~2/3) of water consumption by humans is used for agriculture, where approximately half of all global food

Hydrol. Earth Syst. Sci. Discuss., doi:10.5194/hess-2016-92, 2016
Manuscript under review for journal Hydrol. Earth Syst. Sci.
Published: 2 March 2016

production comes from irrigated agriculture (Mekonnen et al., 2011). As such, an increase in food demand will put an even greater demand on fresh water resources, particularly an increasing reliance on groundwater (Mekonnen et al., 2011). The ability to model and forecast the hydrologic cycle will continue to play a major role in effective water resource management in the coming decades. Currently, most land surface models (LSM) aimed at characterizing the fluxes of water, energy, and nutrients, have relied on either sparse point scale *SWC* monitoring networks (Crow et al. 2012) or remote sensing products with large pixel sizes (~36 km) and shallow penetration depths (e.g., ~ 2-5 cm for SMOS; Kerr et al., 2010 and SMAP Entekhabi et al., 2010). A critical scale gap exists between these methods requiring innovative monitoring strategies (Robinson et al., 2008). Moreover, as LSMs continue to move towards highly refined spatial resolutions of 1 km or less (Wood et al., 2011), the need for accurate and spatially exhaustive *SWC* datasets continues to grow (Beven and Cloke, 2012).

Estimating and monitoring *SWC* at the appropriate spatial and temporal scale for effective incorporation into LSMs has proven to be a difficult task. On one hand, monitoring networks at the regional (e.g., Nebraska Automated Weather Data Network; AWDN, Oklahoma Mesonet) and continental scales (Climate Reference Network; CRN, Soil Climate Analysis Network; SCAN) have continuously recording point sensors. However, these networks have limited spatial coherence due to the nature of point based *SWC* sensors only representing the point at which they are placed, and not the surrounding landscape (Vereecken et al., 2008). Techniques such as temporal stability analysis (Vachaud et al., 1985) can help improve the representativeness of the monitoring networks but require *a priori* spatial information. On the other hand, remote sensing satellites using passive microwaves can monitor global *SWC* data every few days albeit with large spatial footprints (~36 km, Entekhabi et al., 2010; Kerr et al., 2010). In addition, passive

Hydrol. Earth Syst. Sci. Discuss., doi:10.5194/hess-2016-92, 2016
Manuscript under review for journal Hydrol. Earth Syst. Sci.
Published: 2 March 2016

67 microwaves lack significant penetration depths (~ 2-5 cm Njoku et al., 1996), limiting their
68 effectiveness as a remote sensing input for full root zone coverage in LSMs.

69 Alternatively, the field of geophysics offers a variety of techniques to help fill the spatial
70 and temporal gaps between point sensors and remote sensing products (Robinson et al., 2008).
71 Bridging this gap requires both novel geophysical techniques and integrated modeling strategies
72 capable of merging both point and remotely sensed data into a unified framework (Binley et al.,
73 2015). One promising geophysical technique to help fill this need is fixed (Desilets et al., 2010,
74 Zreda et al., 2012) and roving cosmic-ray neutron probes (CRNP; Chrisman et al., 2013, Dong et
75 al., 2014), which measures the ambient amount of low-energy neutrons in the air. The low-
76 energy neutrons are highly sensitive to the mass of hydrogen, and thus *SWC*, in the near surface
77 (Zreda et al., 2012). CRNP estimate the area-average *SWC* because neutrons are well mixed
78 within the footprint of the sensor which typically has a radius of ~300 m and depths of ~12-76
79 cm (Desilets and Zreda 2013, Kohli et al., 2015).

80 To date, the CRNP method has been mostly used as a fixed system in one location to
81 continuously measure *SWC* as part of a large monitoring network (Zreda et al., 2012, Hawdon et
82 al., 2014). Recent advancements have allowed the CRNP to be used in mobile systems to
83 monitor transects across Hawaii (Desilets et al., 2010), monitor entire basins in southern Arizona
84 (Chrisman et al., 2013), compare against remote sensing products in central Oklahoma (Dong et
85 al., 2014), and monitor ~140 agricultural fields in eastern Nebraska (Franz et al., 2015). In order
86 to accurately estimate *SWC*, the CRNP method relies on a calibration function to convert
87 observed low-energy neutron counts into *SWC* (Desilets et al., 2010, Bogena et al., 2013, see
88 Sec. 2.2 for full details). The calibration procedure requires site specific sampling of both soil
89 and vegetation data in order to determine the required parameters. While the calibration of a

Hydrol. Earth Syst. Sci. Discuss., doi:10.5194/hess-2016-92, 2016
Manuscript under review for journal Hydrol. Earth Syst. Sci.
Published: 2 March 2016

fixed CRNP is fairly standardized (Zreda et al., 2012; Franz et al., 2012; Iwema et al., 2015, Baatz et al., 2015), the heterogeneous nature of soil and vegetation characteristics across a landscape makes the pragmatic calibration of the mobile CRNP a significant challenge. Specifically, the presence of water within vegetation and the soil minerals may alter the shape of the local calibration function and thus accuracy of *SWC*. The need for reliable, accurate, depth-dependent, and localized soil and vegetation spatial information for use in the calibration function is critical in order to fully harness the potential of the CRNP to monitor landscape scale *SWC* across the globe.

The objective of this study is to explore the utility and accuracy of currently available global soil and vegetation datasets (soil organic carbon, soil bulk density, soil clay weight percent, and crop biomass) for use in the calibration function. To accomplish our objective, we aimed to answer the following questions:

1) Can global datasets of soil bulk density, soil organic carbon, and soil clay weight percent be used to in lieu of *in-situ* sampling within reasonable error for use in the CRNP calibration function?

2) Can the use of remotely sensed vegetation products, specifically the Green Wide Dynamic Range Vegetation Index (GrWDRVI) be used to quantify fresh biomass with reasonably low error (< 1 kg/m^2) for use in the CRNP calibration function?

To answer these questions, we tested the accuracy of these datasets against *in-situ* sample datasets of the same parameters. Existing *in-situ* datasets from across the CONUS were then combined with *in-situ* datasets from eastern Nebraska, which focused on fast growing crops of maize and soybean. Specifically, we tested the accuracy and use of a ~1 km global soil dataset

Hydrol. Earth Syst. Sci. Discuss., doi:10.5194/hess-2016-92, 2016
Manuscript under review for journal Hydrol. Earth Syst. Sci.
Published: 2 March 2016

(Shangguan et al., 2014). In addition, we examined the use of the Green Wide Dynamic Range Vegetation Index (*GrWDRVI*, Gitelson, 2004) derived from NASA's MODIS sensor aboard the Terra satellite for use in estimating the amount of fresh crop biomass.

The remainder of the paper is organized as follows: In the Methods section, the CRNP method is first presented, with emphasis on the integration of the calibration function and soil and vegetation parameters to convert observed low-energy neutron counts into *SWC*. Next, *in-situ* methods for estimating the soil and vegetation calibration parameters are discussed, which is followed by discussions on the soil and vegetation products available globally at ~1 km resolution. In the Results section, we first compare the *in-situ* soil sampling against the global datasets. Next, we develop a 1 km CONUS soil lattice water map using *in-situ* samples. We then compare the *GrWDRVI* against *in-situ* samples from Nebraska to estimate the changes in maize and soybean fresh biomass. Lastly, we present an error propagation analysis investigating the potential uncertainty of using the global soil calibration data vs. local *in-situ* sampling. The paper concludes with a discussion on best practice recommendations for calibrating and validating a roving CRNP experiment.

2. Methods

2.1 Overview of Cosmic-ray Neutron Probe

The CRNP estimates area-averaged *SWC* via measuring the intensity of epithermal neutrons near the ground surface (Zreda et al. 2008, 2012). A cascade of neutrons with varying energy levels are created in the earth's atmosphere when incoming higher energy particles produced within supernovae interact with atmospheric nuclei (Zreda et al., 2012 and Kohli et al.,

Hydrol. Earth Syst. Sci. Discuss., doi:10.5194/hess-2016-92, 2016
Manuscript under review for journal Hydrol. Earth Syst. Sci.
Published: 2 March 2016

134 2015). After fast neutrons are created, they continue to lose energy during numerous collisions
135 with nuclei in air and soil, and become epithermal neutrons (i.e., the neutrons which are
136 primarily measured by the moderated detector). The abundance of hydrogen atoms in the air and
137 soil largely controls the removal rate of epithermal neutrons from the system (Zreda et al. 2012).
138 Water in the near surface soil (i.e. *SWC*) is one of the largest sources of hydrogen present in
139 terrestrial systems (McJannet et al. 2014). Thus, relative changes in the intensity of epithermal
140 neutrons are overwhelmingly due to changes in the *SWC*. However, the shape of the calibration
141 function (see section 2.2) is modified by local soil and vegetation parameters (Zreda et al. 2012)
142 reflecting the variation of background hydrogen levels across landscapes.

143 Using a standard neutron detector with a 2.54 cm layer of plastic, Zreda et al. (2008) first
144 described the support volume the detector measures to be a circle of ~300 m in radius with
145 vertical penetration depths of 12 to 76 cm depending on *SWC*. Recent neutron transport
146 modeling has further refined the footprint area to be a function of atmospheric water vapor,
147 elevation (Desilets and Zreda, 2013), surface heterogeneity (Kohli et al., 2015), vegetation, and
148 *SWC*. Given the large measurement footprint area at tens of hectares, this non-invasive
149 technique is an ideal complement to long-term surface energy balance monitoring around the
150 globe. Currently, there are >200 fixed CRNP (personal communication with Darin Desilets of
151 HydroInnova LLC, Albuquerque, NM) functioning in this capacity around the United States of
152 America (Zreda et al., 2012), Australia (Hawdon et al., 2014), Germany (Baatz et al., 2015),
153 South Africa, China, and the United Kingdom. The real-time *SWC* data provide critical
154 infrastructure for use in weather forecasting and data assimilation in LSMs (Shuttleworth et al.,
155 2013, Rosolem et al., 2014, Renzullo et al., 2014).

Hydrol. Earth Syst. Sci. Discuss., doi:10.5194/hess-2016-92, 2016
Manuscript under review for journal Hydrol. Earth Syst. Sci.
Published: 2 March 2016

Hydrology and Earth System Sciences
Discussions

156 In addition to the fixed CRNP measuring hourly *SWC*, a roving version of the CRNP has
157 been used to reliably measure *SWC* at temporal resolutions as low as 1 minute (Chrisman et al.,
158 2013; Dong et al., 2014) providing the ability to make *SWC* maps over hundreds of square
159 kilometers in a single day. Moreover, Franz et al. (2015) found that a combination of fixed and
160 roving CRNP data in a statistical framework has the ability to form an accurate, real-time, and
161 multiscale monitoring network. With the continued increase in observation spatial scales, the use
162 of *in-situ* sampling in the traditional CRNP calibration procedure is no longer practical, thus
163 requiring the use of alternative available datasets to improve its operability. The remainder of
164 this work will first describe the availability of such global datasets and then test the accuracy of
165 using the datasets in the CNRP calibration function.

166

167 **2.2 The Cosmic-ray Neutron Probe Calibration Function**

168 In order to convert observed epithermal neutron measurements into *SWC*, a series of
169 correction factors and calibration functions have been developed. Zreda (2012) describes in
170 detail the correction factors needed for geomagnetic latitude, changes in incoming high-energy
171 cosmic-ray intensity, and atmospheric pressure. Rosolem et al. (2013) further describes a
172 correction factor for changes in absolute air humidity near the surface. Following these four
173 correction factors, the corrected epithermal neutron counts can be converted into *SWC*. Desilets
174 et al. (2010) proposed the original calibration function (Eq. 1) valid for mass based gravimetric
175 measurements which Bogena et al. (2013) further expanded for volumetric water content. The
176 calibration function has been successfully tested against direct sampling and point sensor
177 measurements with RMSE < 0.03 cm^3/cm^3 across the globe including arid shrublands in
178 Arizona, USA (Franz et al., 2012), semi-arid forests in Utah, USA (Lv et al., 2014), to humid

Hydrol. Earth Syst. Sci. Discuss., doi:10.5194/hess-2016-92, 2016
Manuscript under review for journal Hydrol. Earth Syst. Sci.
Published: 2 March 2016

Hydrology and Earth System Sciences
Discussions

179 forests in Germany (Bogena et al., 2013), and across ecosystems in Australia (Hawdon et al.,
180 2014). The original calibration function proposed by Desilets et al., (2010) is:

181 $$\theta_T = \left(\frac{a_0}{\frac{N}{N_0} - a_1} - a_2\right) \quad (1)$$

182 where θ_T (g/g) is the total gravimetric water content, a_0 = 0.0808, a_1= 0.3720, a_2 = 0.1150 (see
183 Desilets et al., (2010) for details), N(counts per time interval) is the aforementioned epithermal
184 corrected neutron count rate, and N_0 (counts per time interval) is the theoretical counting rate at a
185 location with dry silica soils. Zreda et al. (2012) illustrated that:

186 $$\theta_T = \theta_p + \theta_{LW} + \theta_{SOC} \quad (2)$$

187 where θ_p (g/g) is the gravimetric pore water content in the soil, θ_{LW} (g/g) is the soil lattice water,
188 and θ_{SOC} (g/g) is the soil organic carbon water equivalent. The volumetric soil water content,
189 SWC, (cm^3/cm^3) is found by multiplying θ_p by $\frac{\rho_b}{\rho_w}$, where ρ_b (g/cm^3) is dry soil bulk density and
190 ρ_w = 1 g/cm^3 is the density of water.

191 To account for effects of time varying above-ground vegetation on the epithermal neutron
192 counts (Franz et al., 2013; Coopersmith et al., 2014), Franz et al. (2015) proposed the following
193 additional correction factor to N_0:

194 $$N_0(BWE) = m * BWE + N_0(0) \quad (3)$$

195 where $N_0(0)$ is the instrument specific estimate of N_0 with no standing biomass, BWE is the
196 biomass water equivalent (kg/m^2 ~ mm of water/m^2), and m is the slope of the relationship
197 between N_0 and BWE, determined via *in-situ* calibration datasets. The BWE is further defined
198 as:

Hydrol. Earth Syst. Sci. Discuss., doi:10.5194/hess-2016-92, 2016
Manuscript under review for journal Hydrol. Earth Syst. Sci.
Published: 2 March 2016

Hydrology and Earth System Sciences
Discussions

$$BWE = SWB - SDB + SDB * f_{WE} \quad (4)$$

where SWB is the standing wet biomass per unit area (kg/m^2 ~ mm of water/m^2), SDB is the standing dry biomass per unit area (kg/m^2 ~ mm of water/m^2), and $f_{WE} = 0.494$ is the stoichiometric ratio of H_2O to organic carbon (assuming organic carbon is cellulose, $C_6H_{10}O_5$). Using nine *in-situ* calibration datasets for maize and soybean crops, Franz et al. (2015) found their roving CRNP had a statistically significant linear relationship between N_0 and BWE yielding $N_0(0) = 518.34$ counts per minute and $m = -4.9506$ (R^2 = 0.515 and p-value = 0.03). We note the coefficients are less suitable for forest canopies given the need for a neutron geometric efficiency factor described further in the supplemental material of Franz et al. (2013). We also refer the reader to Coopersmith et al. (2014) and Baatz et al. (2015) for further discussion of CRNP use in forest canopies.

2.3 *In-situ* Soil and Vegetation Calibration Parameters

The calibration function summarized in equations (1-4) requires depth-average estimates of three soil parameters, θ_{LW}, θ_{SOC}, and ρ_b, and two vegetation parameters SWB and SDB. In order to estimate area-average soil parameters, Zreda et al. (2012) and Franz et al. (2012) recommended averaging 108 individual *in-situ* soil samples from 18 locations (every 60 degrees and radii of 25, 75, 200 m) and six depths (every 5 cm from 0-30 cm) within a CRNP footprint. In light of recent modeling work (Kohli et al. 2015), this sampling pattern may need to be adjusted to be more representative of encountered conditions (such as shorter sampling distances due to reduced footprint area). Zreda et al. (2012) found that a composite sample of 1 g of material gathered from each of the 108 samples was adequate to estimate θ_{LW} and θ_{SOC}. These

Hydrol. Earth Syst. Sci. Discuss., doi:10.5194/hess-2016-92, 2016
Manuscript under review for journal Hydrol. Earth Syst. Sci.
Published: 2 March 2016

composite samples can be analyzed directly for lattice water (g/g), soil total carbon (TC, g/g), and inorganic carbon (TIC, g/g) determined by measuring CO_2 after the sample is acidified (e.g. by Actlabs of Ontario Canada, Analysis Codes: 4E-exploration, 4F-CO2, 4F-C, and 4F-H2O+/-). Franz et al. (2015) reported $\theta_{SOC} = (TC - TIC) * 1.724 * f_{WE}$, where 1.724 is a constant to convert total organic carbon into total organic matter and f_{WE} is given above. To estimate ρ_b at each location, Zreda et al. (2012) used a 30 cm long split tube auger, which contained six 5 cm diameter by 5 cm length rings. All samples were then averaged to get a composite value.

In order to estimate standing wet biomass (*SWB*) and standing dry biomass (*SDB*) in maize and soybeans, Franz et al. (2015) measured average plant density in 1 m^2 quadrats at each of the 18 sampling locations. In a subset of six sites (randomly chosen one radius for each of the six transects) three plants were removed and placed in a paper bag for weighing within two hours (to minimize water loss). The plants were then dried for five days at 70^o C and weighed again. Using the density of plants, wet weight, and dry weight, *SWB* and *SDB* can be determined at each site and averaged across the CRNP footprint.

2.4 Global Datasets of Soil Properties

Shangguan et al. (2014) compiled a thirty arc second (~1 km) Global Soil DatasEt (GSDE) with 34 soil parameters in 8 layers (0–0.045, 0.045–0.091, 0.091–0.166, 0.166–0.289, 0.289–0.493, 0.493–0.829, 0.829–1.383, and 1.383–2.296 m). In order to construct an average value relevant to the CRNP, we arithmetically averaged the top four layers in each grid location to form a composite value (~30 cm) over the CONUS. The GSDE contains estimates of soil bulk density and soil organic carbon. In order to construct a map of lattice water, we explored if any

Hydrol. Earth Syst. Sci. Discuss., doi:10.5194/hess-2016-92, 2016
Manuscript under review for journal Hydrol. Earth Syst. Sci.
Published: 2 March 2016

243 relationships existed between clay weight fraction and lattice water following the work of
244 Greacen et al. (1981) using active neutron probe calibration procedures developed for Australian
245 soils. In order to account for variations in chemical and physical weathering on lattice water
246 (Zreda et al., 2012), we further partitioned the analyses based on soil order. A global soil order
247 map with a resolution of five arc minutes (~ 8 km) containing 25 major soil classifications was
248 first uploaded to ArcMap (ESRI, v. 10.2.2) and clipped to the CONUS. The 25 soil
249 classifications were then categorized into 12 major classifications of U.S. soil taxonomy (see Fig.
250 1, personal communication with Prof. M. Kuzila, University of Nebraska-Lincoln). The
251 reduction from 25 to 12 soil classifications allowed us to generate larger sample sizes for each
252 classification from the available calibration datasets. Using the available lattice water samples
253 from Zreda et al. (2012) and additional samples collected *in-situ* over 2014, we analyzed if any
254 statistically significant relationships existed between GSDE clay weight percent and 61 *in-situ*
255 lattice water samples for each of the US soil orders (Table S1). We note that this procedure could
256 be used globally if *in-situ* lattice water samples were available for all 25 soil taxonomic groups.
257 From these relationships, a map of the CONUS lattice water weight percent was developed by
258 using either the mean value of the *in-situ* lattice water or the linear relationships between clay
259 weight percent (from the GSDE) and the lattice water *in-situ* samples. Additionally, *in-situ*
260 samples of soil organic carbon, bulk density, clay weight percent, and lattice water were
261 compared against the same parameters derived from the GSDE.

262

263 **2.5 Global Datasets of Vegetation Properties**

264 In order to estimate *SWB* and *SDB*, we downloaded remotely sensed 500 m MODIS
265 reflectance data from NASA's Terra satellite (http://earthexplorer.usgs.gov/). To calibrate and

Hydrol. Earth Syst. Sci. Discuss., doi:10.5194/hess-2016-92, 2016
Manuscript under review for journal Hydrol. Earth Syst. Sci.
Published: 2 March 2016

validate the *in-situ* vegetation data to the remotely sensed vegetation estimates, we sampled two different agricultural areas in eastern Nebraska. The MODIS reflectance data were used to generate various vegetation indices (see detailed information below), and then calibrated against historical biomass data (2003-2013) from 3 fields near Mead, NE. Each field is part of the AmeriFlux network (http://ameriflux.ornl.gov/) with data going back to 2001 (site description given in Suyker et al., 2005). Each field is approximately 65 ha. Field 1 (Mead Irrigated/US-Ne1, 41.1650°, -96.4766°) is irrigated with continuous maize. Field 2 (Mead Irrigated Rotation/US-Ne2, 41.1649°, -96.4701°) is irrigated with a rotation of maize and soybean. Field 3 (Mead Rainfed/US-Ne3, 41.1797°, -96.4396°) is rainfed with a rotation of maize and soybean. At these three fields, destructive biomass samples were collected approximately every two weeks at 6 different locations in the field, typically consisting of 30-35 individual plants per sampling bout. From the destructive sampling bouts, we were able to compute *SWB* and *SDB*. The sites, with their long sampling records consisting of both rainfed and irrigated soybean and maize, are an ideal location for calibrating the remote sensing reflectance data and vegetation indices. In order to validate the derived vegetation index and coefficients from the above mentioned three sites, we used 4 bouts of destructive biomass sampling at two fields (each approx. 65 ha.) during 2014 near Waco, NE (Franz et al. 2015). The fields were irrigated maize (40.9482°, -97.4875°) and irrigated soybean (40.9338°, -97.4587°). *SWB* and *SDB* were collected following the protocol described in section 2.3.

A total of 924 MODIS images over the growing seasons (May to October) between 2003 and 2014 were downloaded for calibration and validation of the corresponding destructive biomass samples at the five field sites in central and eastern Nebraska (note: MODIS images from the closest date to *in-situ* sampling were used with up to a 4 day offset). Using the Python

Hydrol. Earth Syst. Sci. Discuss., doi:10.5194/hess-2016-92, 2016
Manuscript under review for journal Hydrol. Earth Syst. Sci.
Published: 2 March 2016

289 Integrated Development Environment (v. 2.7.8) built into ArcGIS (v. ESRI, v. 10.2.2), we
290 extracted the MODIS reflectance data in the green and near-infrared electromagnetic spectrum
291 range. Next, we removed any pixels that were skewed by incidental cloud cover (Nguy-
292 Robertson & Gitelson, 2015). The resulting data were then transformed from separate reflectance
293 images into the Green Wide Dynamic Range Vegetation Index (*GrWDRVI*; Gietelson, 2004):

294 $$GrWDRVI = \frac{(0.1 * Near\ Infrared - Green)}{(0.1 * Near\ Infrared + Green)} \quad (5)$$

295 where near-infrared light (MODIS band 2) has wavelength between 841 and 876 nm and green
296 light (MODIS band 4) has wavelength between 545 and 565 nm. The *GrWDRVI* has been shown
297 to have better correlations with observed *in-situ* biomass as compared to other vegetation indices
298 such as NDVI (Nguy-Robertson et al., 2012; Nguy-Robertson & Gitelson, 2015). We then
299 investigated if any relationships existed between *GrWDRVI* and *SWB* and *SDB*.

300

301 **2.6 Error Propagation Analysis of GSDE Soil Properties**

302 We used a Monte Carlo analysis to estimate the expected uncertainty if the GSDE
303 parameters were used instead of *in-situ* estimates. The statistical metrics of root mean square
304 error (RMSE), mean absolute error (MAE), and bias were used to describe the error propagation
305 in the Monte Carlo simulation experiment. Using the 61 CONUS *in-situ* samples and the GSDE
306 soil properties, we estimated the mean difference and the covariance matrix for θ_{LW}, θ_{SOC}, and
307 ρ_b. Using these data, we simulated 100,000 realizations of the "true" (i.e. from the *in-situ*
308 sampling) and perturbed soil properties using a multivariate normal distribution. Using a range of
309 observed neutron counts and solving equations (1-2) with the true and perturbed soil properties,
310 we also estimated the true and perturbed *SWC*. In order to provide realistic constraints on the

Hydrol. Earth Syst. Sci. Discuss., doi:10.5194/hess-2016-92, 2016
Manuscript under review for journal Hydrol. Earth Syst. Sci.
Published: 2 March 2016

311 error propagation results, we assumed soil bulk density was constrained between 1.2-1.5 g/cm^3,
312 lattice water between 1-8 wt. %, soil organic carbon between 0-8 wt. %, and *SWC* between 0.03-
313 0.45 cm^3/cm^3. Simulated and calculated values outside of these bounds were either reset to the
314 minimum or maximum value or removed from the Monte Carlo statistics. A minimum threshold
315 of 70% of simulated cases was used to compute all error statistics for each case. We note that the
316 effects of growing biomass were not included here given the lack of available calibration datasets
317 at all sites, but could be incorporated in future work following a similar methodology.

318

319 **3. Results**

320 **3.1. Comparison of *In-situ* and Global Soil Calibration Parameters**

321 The comparisons between observed clay weight percent, soil bulk density, soil organic
322 carbon and the GSDE values are summarized in Table S1 and Figure 2 a, b, c for the 61
323 sampling sites within the CONUS. Other than 1 outlier (south central Texas, 29.9492^o, -
324 97.9966^o, which is located on the border between vertisols and alfisol soils), the comparison
325 between the mean observed and GSDE clay weight percent (of sites that had clay weight
326 percent) behaved well (RMSE = 5.45 wt. %, R^2 = 0.68) considering the difference in scale and
327 methods. The comparisons between soil bulk density (RMSE = 0.173 g/cm^3, R^2 = 0.203) and soil
328 organic carbon as it was during the various 2011-2014 sampling campaigns, (RMSE = 1.47 wt.
329 %, R^2 = 0.175) generally followed the same positive trend.

330 In order to construct a map of the CONUS lattice water, we investigated if any significant
331 relationships existed between GSDE clay wt. % and observed lattice water for each US soil
332 taxonomic group (Table 1) following the relationships described from observations in Australian

Hydrol. Earth Syst. Sci. Discuss., doi:10.5194/hess-2016-92, 2016
Manuscript under review for journal Hydrol. Earth Syst. Sci.
Published: 2 March 2016

Hydrology and Earth System Sciences
Open Access
Discussions

soils (Greacen, 1981). We found that a significant linear relationship existed between clay wt. % and lattice water for all 61 sites (R^2 = 0.183, p value <0.001). However, after partitioning the sites into soil taxonomic groups, only the mollisol taxonomic group yielded a statistically significant relationship (R^2 = 0.539, p value <0.001). Therefore, in order to construct a CONUS lattice water map, we used the mean values for six taxonomic groups and neglected the remaining five taxonomic groups due to an inadequate number of samples (Figure 3). Figure 2d illustrates the comparison between the derived and observed lattice water for the 61 CONUS sites (RMSE = 1.299 wt. %, R^2 = 0.315). Table S1 summarizes the observed and GSDE values for all 61 sites and Table 2 summarizes the mean difference and covariance matrix between the *in-situ* values and GSDE values. The mean difference and covariance differences were used in the error propagation analysis described in section 2.6 and 3.3. We note that each of the mean differences followed a normal distribution (see Table S1 for *in-situ* and GSDE values).

3.2. Comparison of *In-situ* and Remotely Sensed Vegetation Calibration Parameters

Using the 11 years of destructive vegetation sampling from 3 fields near Mead, NE, we found that the *GrWDRVI* was able to predict *SWB* when partitioning the data into maize and soybean, irrigated and rainfed, and green-up/mature and senescence periods of crop development (Figure 4 and Tables S2 and S3). Figure 3a and 3b illustrate the logistic functions that were used to predict *SWB* for maize green-up (RMSE = 0.88 kg/m^2) and soybean green-up (RMSE = 0.47 kg/m^2). We note that *SWB* relationships with *GrWDRVI* indicate that *GrWDRVI* values less than 0.25 equated to the absence of *SWB*. During senescence, we found that a second order power law function fit the data well. We found the maize senescence functions (DOY> 210) needed to be further partitioned by irrigated and rainfed conditions as limitations in soil water will occur more

Hydrol. Earth Syst. Sci. Discuss., doi:10.5194/hess-2016-92, 2016
Manuscript under review for journal Hydrol. Earth Syst. Sci.
Published: 2 March 2016

356 quickly with mature plants that utilize the entire root zone. The resulting functions for irrigated
357 maize during senescence (RMSE = 0.75 kg/m^2) and rainfed maize during senescence (RMSE =
358 0.92 kg/m^2) behaved well. For the soybean senescence function (DOY>230), we found a single
359 function behaved reasonably well for both irrigated and rainfed conditions (RMSE = 0.45
360 kg/m^2). As expected from previous research (Ciganda et al, 2008; Peng et al. 2011), we found
361 that the *GrWDRVI* was a poor predictor of *SDB*/percent water content of the vegetation. We will
362 discuss these reasons and alternative strategies for estimating *SDB* in section 4.2.

363 Using the derived relationships from the three study sites near Mead, NE, we applied the
364 equations to our two study sites near Waco, NE (~ 88 km from Mead, NE, Figure 5 and Tables 3
365 and 4). Figure 5 illustrates the time series of *SWB* using the 8 day MODIS product and derived
366 equations for both field sites. The figure also illustrates the observed destructive sampling for 4
367 different sampling bouts. With the limited data, we found the time series of *SWB* calculated from
368 the MODIS data followed the expected green-up and senescence *SWB* behavior for both the
369 irrigated maize and soybean. The *GrWDRVI* derived *SWB* largely captured the maximum
370 observed value for both the irrigated maize (6.58 kg/m^2 vs. 6.2 kg/m^2) and irrigated soybean
371 (2.61 kg/m^2 vs. 1.81 kg/m^2). The largest discrepancy was during the maize green-up period
372 (DOY 183) where the observed value was 2.4 kg/m^2 and ~4.0 kg/m^2 calculated from the
373 *GrWDRVI*. While the derived equations behaved well for this limited validation dataset, the
374 equations should be tested at additional sites where other crop and soil types may influence the
375 function coefficients. Overall, the equations and regression fits resulting in RMSE < 1 kg/m^2 are
376 within the uncertainty of destructive biomass sampling in crops (Franz et al., 2013; 2015). By
377 having general *SWB* relationships (for eastern Nebraska) through time using the 8 day MODIS

Hydrol. Earth Syst. Sci. Discuss., doi:10.5194/hess-2016-92, 2016
Manuscript under review for journal Hydrol. Earth Syst. Sci.
Published: 2 March 2016

data, this could allow for reasonable biomass corrections to N_0 with minimal effects (<0.01 cm^3/cm^3) on the overall estimation of *SWC*.

3.3. Error Propagation Analysis of GSDE Soil Properties

In order to further assess the accuracy of our datasets, we synthetically altered the parameters via a Monte Carlo error analysis. This was done using the GSDE soil parameters (θ_{LW}, θ_{SOC}, and ρ_b) as compared to using local sampling (Figure 6). The analysis revealed that for the given bounds of θ_{LW}, θ_{SOC}, and ρ_b, the maximum RSME was around 0.035 cm^3/cm^3 at a *SWC* = 0.40 cm^3/cm^3. The asymmetric shape of all the curves is expected given the nonlinear calibration function in Eq. (4) and the bounded nature of soil moisture. We found that ρ_b was by far the most sensitive parameter, followed by θ_{LW} and then θ_{SOC}. We expect the influence of vegetation changes to be small on the overall accuracy of *SWC* (<0.01 cm^3/cm^3) given the low RMSE described in section 3.2 (< 1 kg/m^2, which is ~1 mm of water or 0.0033 cm^3/cm^3 for a soil depth of 300 mm). We also note the critical factor in the error propagation analysis is the assumed range of ρ_b, given that it is directly multiplied by the gravimetric water content in the calibration function. *Therefore, future sampling efforts or evaluations of available datasets should seek to minimize the range of bulk density.*

4. Discussion

4.1. Global Soil Calibration Parameters

Hydrol. Earth Syst. Sci. Discuss., doi:10.5194/hess-2016-92, 2016
Manuscript under review for journal Hydrol. Earth Syst. Sci.
Published: 2 March 2016

398 The correlation between observed and GSDE clay content was very strong (Figure 2a) for
399 all 61 sites in the CONUS except for the site in south central Texas. The site occurred near a
400 transition from vertisol to alfisol soil taxonomic groups; the site may have been improperly
401 categorized (Table S1) or may have straddled a sharp gradient in clay contents. The strong
402 correlation of the GSDE clay content with the observed values allowed us to use the GSDE clay
403 content in understanding the correlation between clay content and lattice water organized by US
404 soil taxonomic groups (Table 1). A strong correlation was only found for clay content and lattice
405 water for the mollisol soil taxonomic group (see Greacen, 1981; Zreda et al., 2012). This strong
406 correlation is significant because large portions of the Midwest and Great Plains regions of the
407 United States are made up of mollisol soils. Globally, mollisol soils comprise about 7% of the
408 land surface (United Nations 2007) but contain some of the highest productive grassland and
409 crop areas (i.e. Central USA, Argentina, Central Eurasia). As such, the roving CRNP method
410 remains applicable within grassland agricultural settings. No significant linear relationships with
411 clay content were found for alfisol, aridisol, entisol, inceptisol, spodosol, or ultisol. Instead the
412 mean value was assigned to the alfisol, aridisol, entisol, inceptisol, spodosol, and ultisol soil
413 taxonomic groups when generating the CONUS map. We found the differences in most of the
414 soil taxonomic mean values were statistically significant among different taxonomic groups
415 given the small standard errors of the means (not shown but can be calculated from data in Table
416 1). The current analysis did not contain enough samples for the soil taxonomic groups of andisol,
417 gelisol, histosol, oxisol, or vertisol to perform a linear regression or assign a mean value. We
418 recommend future work to consider repeating the analysis for a larger dataset using the FAO
419 2007 (United Nations 2007) soil classification of all 25 groups (also classified for our sites in
420 Table S1). Given the widespread interest in both the fixed and roving cosmic-ray technology, a

Hydrol. Earth Syst. Sci. Discuss., doi:10.5194/hess-2016-92, 2016
Manuscript under review for journal Hydrol. Earth Syst. Sci.
Published: 2 March 2016

421 database of lattice water and clay content for each site could be developed. In addition,
422 warehouses like the Natural Resources Conservation Service (NRCS) in Lincoln, NE contain
423 stored samples from around the USA. This warehouse with others around the globe could be
424 further sampled to help complete the global dataset for use by the cosmic-ray community.
425 Finally, the NRCS regularly updates the Soil Survey Geographic Database (SSURGO), which
426 contains higher spatial resolution and vertically resolved estimates of soil texture and structure
427 (i.e. clay content and bulk density). With the defined regression relationships and soil taxonomic
428 groups, better spatial maps of lattice water could be generated. This may become important for
429 applications of the rover at scales less than 1 km, such as using it for applications in precision
430 agriculture.

431 The correlation between the observed and GSDE soil organic carbon was fairly poor,
432 particularly at the high end (> 4 wt. %). The history of land use is critical in determining carbon
433 pools and how they change through time (Post et al., 2000) and may not be well represented in
434 the GSDE. However, we note that organic carbon has a relatively small impact on the calibration
435 function as it is multiplied by several factors in the calibration equation. For rover survey
436 experiments, we suggest that this be sampled with composite samples, particularly between sites
437 with varying land use histories which can be identified using historical land cover maps.

438 Observed *in-situ* soil bulk density and GSDE bulk density exhibited a positive
439 relationship, albeit with low R^2. The poor fit and sensitivity of the parameter in the calibration
440 function increases the importance of identifying the range and variability of bulk density within
441 the rover sample domain. The variability shown here by the standard deviation of the bulk
442 density for the individual point samples within the 28 ha sample domain varied between 0.1 and
443 0.2 g/cm^3. Moreover, minimizing the expected range of bulk density at a site is key given the

Hydrol. Earth Syst. Sci. Discuss., doi:10.5194/hess-2016-92, 2016
Manuscript under review for journal Hydrol. Earth Syst. Sci.
Published: 2 March 2016

444 propagation of error analysis presented in section 3.3. Thus, this result supports direct sampling
445 at key locations (along gradients of land use, soil taxonomic groups, etc.) to constrain the range
446 of expected bulk density values. We also suggest that for rover surveys in the USA (and
447 elsewhere), additional higher resolution datasets like SSURGO be used instead of the 1 km
448 GSDE (in particular bulk density data as a function of depth), as significant small scale
449 variability may be averaged out. This may be critical to account for in future roving CRNP
450 research areas, such as precision agriculture or small scale watershed monitoring where
451 significant soil texture variation may exist at short length scales.

452

453 **4.2. Global Remotely Sensed Vegetation Calibration Parameters**

454 The comparison of 11 years of destructive vegetation samples from maize and soybeans
455 at 3 sites in eastern Nebraska indicated that the *GrWDRVI* was able to predict *SWB* in
456 agricultural fields, especially when partitioned into green-up vs. senescence and irrigated vs.
457 rainfed (Figure 4). However, as expected the *GrWDRVI* was unable to predict *SDB*. The main
458 reason is as the plants begin to dry out during the late summer and early fall, leaves lose their
459 chlorophyll and leaf structure beings to collapse thereby increasing reflected green and reducing
460 near-infrared light (Ciganda et al. 2008; Peng et al. 2011). This is exaggerated by a change in the
461 allocation of resources by the plant from leaves to grain, shifting where the majority of mass is
462 located and thus weakening the capacity for the *GrWDRVI* to predict *SDB*. This biological
463 investment of resources is more pronounced for maize than soybeans. As additional crops are
464 included in this analysis, the location and development of the fruit and seed will impact the
465 predictive relationships using vegetation indices.

Hydrol. Earth Syst. Sci. Discuss., doi:10.5194/hess-2016-92, 2016
Manuscript under review for journal Hydrol. Earth Syst. Sci.
Published: 2 March 2016

While the developed regression relationships for maize and soybean (Table S3) were tested against independent biomass estimates from Waco, NE (Figure 5), we note that further validation is needed. In terms of a strategy for estimating *SDB*, we suggest that proxies such as crop type and growth stage be used. Franz et al. (2013 and 2015) found that in early stages, maize and soybean had canopy water contents from 75-90 wt. %. By the end of senescence before harvest, the canopy water contents were down to 25-35 wt. %. If growth stage is not directly known, local meteorological observations, planting date, and crop variety can be used to compute proxies (e.g. growing degree days) or simulated from crop models (Allen et al. 1998). We note that having a reasonably accurate estimate of *SWB* and thus *BWE* (within ~ 1 kg/m^2) is all that is required to have a relatively small impact (< 0.01 cm^3/cm^3) on the estimated *SWC*. Finally, we note that this methodology is not applicable to areas with woody biomass. Following Franz et al., (2013), Hawdon et al., (2014), Baatz et al., (2015), and Coopersmith et al., (2014) we suggest other vegetation relationships (i.e. *BWE* vs. N_0) be defined. However, given the relatively small changes in *BWE* over the year in forests, we would expect small changes in N_0 through time.

5. Summary and Conclusions

In this work, we developed a framework using globally available datasets for estimating four (θ_{LW}, θ_{SOC}, ρ_b, SWB) of the five key soil and vegetation parameters needed by the cosmic-ray neutron method for estimating *SWC* in fast growing vegetation areas such as row crop production in agricultural areas. The remaining crop vegetation parameter (*SDB*) can be fairly well approximated by crop type, growth stage or simulated with crop models. The accuracy of the GSDE soil database was tested against 61 calibration datasets from the CONUS. We found

Hydrol. Earth Syst. Sci. Discuss., doi:10.5194/hess-2016-92, 2016
Manuscript under review for journal Hydrol. Earth Syst. Sci.
Published: 2 March 2016

that the 1 km GSDE compares well against observed clay content ($R^2 = 0.68$) but much poorer against soil bulk density ($R^2 = 0.203$) and soil organic carbon ($R^2 = 0.175$). Surprisingly, of the six soil taxonomic groups we investigated, only mollisols showed a statistically significant correlation with clay content. The remaining five soil taxonomic groups we investigated did show statistically significant different mean values. These mean values were used to generate a map (not complete) of lattice water for the CONUS. From 11 years of destructive sampling of maize and soybean fields in eastern Nebraska, we found that the 8-day 500 m resolution MODIS derived *GrWDRVI* was highly correlated to *SWB*, particularly when partitioning the fields into green-up vs. senescence and irrigated vs. rainfed (RMSE < 1 kg/m^2). A propagation of error analysis indicated that the range of bulk density values was the most sensitive calibration parameter. For the selected ranges, we found the GSDE vs. local sampling resulted in a maximum RMSE of 0.035 cm^3/cm^3 at a *SWC* = 0.40 cm^3/cm^3.

With the continuing use of the roving CNRP we make the following recommendations on best calibration and use:

1) Collect a series (minimum of 7) of full calibration datasets (θ_{LW}, θ_{SOC}, ρ_b, SWB, SDB) in differing land use and soil types to estimate the instrument specific slope and intercept for correction factor N_0.
2) In the rover sampling area, construct a map of land use including: vegetation/crop type, planting date, variety, rainfed vs. irrigated, and gravel vs. paved roads vs. natural areas.
3) Collect a series of aggregate soil samples for soil organic carbon and lattice water around the survey area. The samples should be collected across land use, soil texture, and soil taxonomic groups. The GSDE or more local datasets like SSURGO in the USA can be used to select sites, cross validate samples, and fill in missing areas.

Hydrol. Earth Syst. Sci. Discuss., doi:10.5194/hess-2016-92, 2016
Manuscript under review for journal Hydrol. Earth Syst. Sci.
Published: 2 March 2016

4) Soil bulk density is the critical parameter in the calibration equations and overall accuracy of the cosmic-ray neutron method. Bulk density should be collected locally wherever possible. More local datasets like SSURGO in the USA will likely perform better at smaller scales than the 1 km GSDE.
5) *SWC* validation datasets should be collected to independently assess the accuracy of the rover survey results.

Acknowledgments

This research is supported financially by the Daugherty Water for Food Institute at the University of Nebraska, NSF EPSCoR FIRST Award, the Cold Regions Research Engineering Laboratory through the Great Plains CESU, and an USGS104b grant. We would also like to thank Chase Johnson and Romher Farms for providing access to field sites, Gary Womack and Darin Desilets for support with the rover, and Mark Kuzila for assistance with soil taxonomy. CONUS 1 km soil datasets for this work can be requested from the corresponding author. We sincerely appreciate the support and the use of facilities and equipment provided by the Center for Advanced Land Management Information Technologies, School of Natural Resources and data from Carbon Sequestration Program, the University of Nebraska-Lincoln.

References

Allen, R. G., L. S. Pereira, D. Raes, and M. Smith, Crop evapotranspiration. Guidelines for Computing Crop Water Requirements. FAO Irrigation and Drainage Paper 56., Food and Agriculture Organization of the United Nations, Rome, Italy. 1998.

534 Baatz R., Bogena H. R., Hendricks Franssen H. J., Huisman J. A., and Montzka C. An Empirical
535 Vegetation Correction for Soil Water Content Quantification Using Cosmic Ray
536 Probes, *Water Resources Research*, Vol. 51, No.4, Pgs. 2030-2046, 2015.
537 Beven K. J., and Cloke H. L. Comment on "Hyperresolution global land surface modeling:
538 Meeting a grand challenge for monitoring Earth's terrestrial water" by Eric F. Wood et
539 al., *Water Resour. Res.*, Vol. 48, W01801, doi:10.1029/2011WR010982, 2012.
540 Binley A., Hubbard S. S., Huisman J. A., Revil A., Robinson D. A., Singha K., and Slater L. D.:
541 The Emergence of Hydrogeophysics for Improved Understanding of Subsurface
542 Processes Over Multiple Time Scales, *Water Resour. Res.*, Vol. 51,
543 doi:10.1002/2015WR017016, 2015.
544 Bogena H. R., Huisman J. A., Baatz R., Hendricks Frassen H. J., and Vereecken H.: Accuracy
545 of the Cosmic-Ray Soil Water Content Probe in Humid Forest Ecosystems: The Worst
546 Case Scenario, *Water Resour. Res.*, Vol. 49, Pgs. 5778-5791, doi:10.1002/wrcr.20463,
547 2013.
548 Chrisman B. B. and M. Zreda: Quantifying Mesoscale Soil Moisture with the Cosmic-Ray
549 Rover, *Hydrology and Earth System Sciences*, Vol. 17, No. 12, Pgs. 5097 – 5108, 2013.
550 Ciganda, V., Gitelson, A.A., and Schepers, J. Vertical Profile and Temporal Variation of
551 Chlorophyll in Maize Canopy: Quantitative "Crop Vigor" Indicator by Means of
552 Reflectance-Based Techniques, *Agronomy Journal*, Vol. 100, No. 5, Pgs. 1409-1417,
553 doi:10.2134/agronj2007.0322, 2008.
554 Coopersmith E. J., Cosh M. H., and Daughtry C. S. T.: Field-Scale Moisture Estimates using
555 COSMOS Sensors: A Validation Study with Temporary Networks and Leaf-Area

Indices, *Journal of Hydrology*, Vol. 519, Part A, Pgs. 637-643, http://dx.doi.org/10.1016/j.jhydrol.20 14.07.060, 2014.

Crow, W. T., A. A. Berg, M. H. Cosh, A. Loew, B. P. Mohanty, R. Panciera, P. de Rosnay, D. Ryu, and J. P. Walker: Upscaling Sparse Ground-Based Soil Moisture Observations For The Validation Of Coarse-Resolution Satellite Soil Moisture Products. *Rev. Geophys*. 50. doi:10.1029/2011rg000372, 2012.

Dane, J. H., and C. G. Topp. Methods of Soil Analysis: Part 4 Physical Methods. Soil Science Society of America. Madison, WI. 2002.

Desilets D., and Zreda M.: Footprint Diameter for a Cosmic-Ray Soil Moisture Probe: Theory and Monte Carlo Simulations, *Water Resour. Res*., Vol. 49, Pgs. 3566–3575, doi:10.1002/wrcr.20187, 2013.

Desilets D., Zreda M., Ferre T. P. A.: Nature's Neutron Probe: Land Surface Hydrology at an Elusive Scale with Cosmic-Rays, *Water Resour. Res*., Vol. 56, doi:10.1029/2009wr008726, 2010.

Dong J. N., Ochsner T. E., Zreda M., Cosh M. H., and Zou C. B.: Calibration and Validation of the COSMOS Rover for Surface Soil Moisture Measurement, *Vadose Zone J.*, Vol. 13, No. 4, doi:10.2136/vzj2013.08.0148, 2014.

Entekhabi D., Njoku E. G., Neill P. E., Kellogg K. H., Crow W. T., Edelstein W. N., and Kimball J.: The Soil Moisture Active Passive (SMAP) Mission, *Proceedings of the IEEE*, Vol. 98, No. 5, Pgs. 704-716, 2010.

Franz T. E., Wang T., Avery W., Finkenbiner C., and Brocca L.: Combined Analysis of Soil Moisture Measurements from Roving and Fixed Cosmic-Ray Neutron Probes for

578 Multiscale Real-Time Monitoring, *Geophys. Res. Lett*., Vol. 42, doi:10.1002/
579 2015GL063963, 2015.
580 Franz T. E., Zreda M., Ferre P. A., Rosolem R., Zweck C., Stillman S., Zeng X., and Shutt W. J.:
581 Measurement Depth of The Cosmic-Ray Soil Moisture Probe Affected by Hydrogen
582 From Various Sources. *Water Resour. Res.*, Vol. 48, (in press), doi:
583 10.1029/2012WR011871, 2012.
584 Franz T. E., Zreda M., Rosolem R., Hornbuckle B. K., Irvin S. L., Adams H., Kolb T. E., Zweck
585 C., and Shuttleworth W. J.; Ecosystem-Scale Measurements of Biomass Water using
586 Cosmic-ray Neutrons, *Geophysical Research Letters*, Vol. 40, Pgs. 1–5,
587 doi:10.1002/grl.50791, 2013.
588 Gietelson, A.A., Wide Dynamic Range Vegetation Index for Remote Quantification of
589 Biophysical Characteristics of Vegetation, Journal of Plant Physiology, Vol. 161, Pgs.
590 165-173, 2004.
591 Greacen, E.L.: Soil water assessment by the neutron method, Australia: CSIRO. 1981.
592 Hawdon A., McJannet D., and Wallace J.: Calibration and Correction Procedures for Cosmic-
593 Ray Neutron Soil Moisture Probes Located Across Australia, *Water Resour. Res*., Vol.
594 50, Pgs. 5029–5043, doi:10.1002/2013WR015138, 2014.
595 Iwema J., Rosolem R., Baatz R., Wagener T., and Bogena H. R.: Investigating Temporal Field
596 Sampling Strategies for Site-Specific Calibration Of Three Soil Moisture-Neutron
597 Intensity Parameterization Methods, *Hydrol. Earth Syst. Sci. Discuss.,* Vol. 12, Pgs.
598 2349-2389. doi:10.5194/hessd-12-2349-2015\, 2015.

599 Kerr Y. H., Waldteufel P., Wigneron J. P., Delwart S., Cabot F. O., Boutin J., and Juglea S. E.:
600 The SMOS Mission: New Tool for Monitoring Key Elements of the Global Water Cycle,
601 *Proceedings of the IEEE*, Vol. 98, No. 5, Pgs. 666-687, 2010.

602 Köhli M., Schrön M., Zreda M., Schmidt U., Dietrich P., and Zacharias S.: Footprint
603 Characteristics Revised for Field-Scale Soil Moisture Monitoring with Cosmic-Ray
604 Neutrons, Water *Resources Research*. doi: 10.1002/2015WR017169, 2015.

605 Lv L., Franz T. E., Robinson D. A., and Jones S. B.: Measured and Modeled Soil Moisture
606 Compared with Cosmic-Ray Neutron Probe Estimates in a Mixed Forest, *Vadose Zone*
607 *Journal*, Vol. 13, No. 12, 2014.

608 McJannet D., Franz T. E., Hawdon A., Boadle D., Baker B., Almeida A., Silberstein R., Lambert
609 T., and Desilets D.: Field Testing of the Universal Calibration Function for
610 Determination of Soil Moisture With Cosmic-Ray Neutrons, *Water Resour. Res.,* Vol.
611 50, Pgs. 5235–5248, doi:10.1002/2014WR015513, 2014.

612 Mekonnen M. M. and Hoekstra A. Y.: The Green, Blue and Grey Water Footprint of Crops and
613 Derived Crop Products, *Hydrol. Earth Syst. Sci*., Vol. 15, Pgs. 1577-1600,
614 doi:10.5194/hess-15-1577-2011, 2011.

615 Nguy-Robertson A., Gitelson A., Peng Y., Viña A., Arkebauer T., and Rundquist D.: Green
616 Leaf Area Index Estimation in Maize and Soybean: Combining Vegetation Indices to
617 Achieve Maximal Sensitivity, *Agronomy Journal*, Vol. 104, No. 5,
618 doi:10.2134/agronj2012.0065, 2012.

619 Nguy-Robertson, A.L., and Gitelson, A.A.: Algorithms for estimating green leaf area index in C3
620 and C4 crops for MODIS, Landsat TM/ETM+, MERIS, Sentinel MSI/OLCI, and Venus

621 sensors, *Remote Sensing Letters*, Vol. 6, No. 5, doi: 10.1080/2150704X.2015.1034888,
622 2015.

623 Njoku E. G., and Entekhabi, D.: Passive Microwave Remote Sensing of Soil Moisture, *Journal of*
624 *Hydrology*, Vol. 184, No. 1, Pgs. 101-129, 1996.

625 Peng, Y., Gitelson, A.A., Keydan, G., Rundquist, D.C., and Moses, W. Remote Estimation of
626 Gross Primary Production in Maize and Support for a New Paradigm Based on Total
627 Crop Chlorophyll Content, *Remote Sensing of Envirionment*, Vol. 115, Pgs. 978-989,
628 doi:10.1016/j.rse.2010.12.001, 2011.

629 Post W. M., and Kwon K. C.: Soil Carbon Sequestration and Land-Use Change: Processes and
630 Potential, *Global Change Biology*, Vol. 6, Pgs. 317-327, doi:10.1046/j.1365-
631 2486.2000.00308.x, 2000.

632 Renzullo L. J., van Dijk A. I. J. M., Perraud J. M., Collins D., Henderson B., Jin H., Smith A. B.,
633 and McJannet D. L.: Continental Satellite Soil Moisture Data Assimilation Improves
634 Root-Zone Moisture Analysis for Water Resources Assessment, *Journal of Hydrology*,
635 Vol. 519, Part D, Pgs. 2747-2762, 2014.

636 Robinson D. A., Binley A., Crook N., Day-Lewis F. D., Ferre T. P. A., Grauch V. J. S., Knight
637 R., Knoll M., Lakshmi V., Miller R., Nyquist J., Pellerin L., Singha K., and Slater L.:
638 Advancing Process-Based Watershed Hydrological Research using Near-Surface
639 Geophysics: A Vision for, and Review of, Electrical and Magnetic Geophysical
640 Methods, *Hydrol. Processes*, Vol. 22, No. 18, Pgs. 3604-3635, 2008a

641 Rosolem, R., W. J. Shuttleworth, M. Zreda, T. E. Franz, X. Zeng, and S. A. Kurc. The Effect of
642 Atmospheric Water Vapor on the Cosmic-ray Soil Moisture Signal. J. Hydrometeorol.
643 doi:10.1175/JHM-D-12-0120.1. 2013.

644 Rosolem R., Hoar T., Arellano A., Anderson J. L., Shuttleworth W. J., Zeng X., and Franz T. E.:
645 Translating Aboveground Cosmic-Ray Neutron Intensity to High-Frequency Soil
646 Moisture Profiles at Sub-Kilometer Scale, *Hydrol. Earth Syst. Sci*., Vol. 18, Pgs. 4363-
647 4379, doi:10.5194/hess-18-4363-2014, 2014.

648 Shangguan W., Dai Y., Duan Q., Liu B., and Yuan H.: A global Soil Dataset for Earth System
649 Modeling, *J. Adv. Model Earth Syst*., Vol. 6, Pgs. 249-263, doi:10.1002/2013MS000293,
650 2014.

651 Shuttleworth J., Rosolem R., Zreda M., and Franz T. E.: The Cosmic-Ray Soil Moisture
652 Interaction Code (COSMIC) for use in Data Assimilation, *Hydrol. Earth Syst. Sci.*, Vol.
653 17, Pgs. 3205-3217, doi:10.5194/hess-17-3205-2013, 2013.

654 Suyker A. E., Verma S. B., Burba G. G., and Arkebauer T. J.: Gross Primary Production and
655 Ecosystem Respiration of Irrigated Maize and Irrigated Soybean During a Growing
656 Season, *Agricultural Forest Meteorology*, Vol. 131, PGs. 180-190, 2005

657 United Nations Department of Economic and Social Affairs (United Nations). World Population
658 Prospects: The 2015 Revision.

659 United Nations Food and Agriculture Organization (FAO). How to Feed the World in 2050,
660 High *Level Expert Forum*, Rome, Italy, 2009.

Hydrol. Earth Syst. Sci. Discuss., doi:10.5194/hess-2016-92, 2016
Manuscript under review for journal Hydrol. Earth Syst. Sci.
Published: 2 March 2016

661 United Nations Food and Agriculture Organization (United Nations). IUSS Working Group WRB,
662 World Reference Base for Soil Resources 2006, first update 2007. World Soil Resources
663 Reports No. 103. FAO, Rome.

664 Vachaud G., Silans A. P. D. E., Balabanis P., Vauclin M.: Temporal Stability of Spatially
665 Measured Soil Water Probability Density Function, *Soil Science Society of America*
666 *Journal*, Vol. 49, Pgs. 822-828, 1985.

667 Vereecken H., Huisman J. A., Bogena H., Vanderborght J., Vrugt J. A., and Hopmans J. W.: On
668 the Value of Soil Moisture Measurements in Vadose Zone Hydrology: A Review, *Water*
669 *Resources Research*, Vol. 44, doi:10.1029/2008wr006829, 2008.

670 Viña A., Gitelson A. A., Nguy-Robertson A. L., and Peng Y.: Comparison of Different
671 Vegetation Indices for the Remote Assessment of Green Leaf Area Index of
672 Crops, *Remote Sensing of Environment*, Vol. 115, No. 12, Pgs. 3468-3478, 2011.

673 Wood E. F., Roundy J. K., Troy T. J., van Beek L. P. H., Bierkens M. F. P., Blyth E., de Roo A.,
674 Döll P., Ek M., Famiglietti J., Gochis D., van de Giesen N., Houser P., Jaffé P. R., Kollet
675 S., Lehner B., Lettenmaier D. P., Peters-Lidard C., Murugesu S., Sheffield J., Wade A.,
676 and Whitehead P.: Hyperresolution Global Land Surface Modeling: Meeting a Grand
677 Challenge for Monitoring Earth's Terrestrial Water, *Water Resources Research*., Vol. 47,
678 doi:10.1029/2010WR010090, 2011.

679 Zreda M., Desilets D., Ferre T. P. A., and Scott R. L.: Measuring Soil Moisture Content Non-
680 Invasively at Intermediate Spatial Scale Using Cosmic-Ray Neutrons, *Geophys. Res.*
681 *Lett.*, Vol. 35, No. 21, doi:10.1029/2008gl035655, 2008.

Hydrol. Earth Syst. Sci. Discuss., doi:10.5194/hess-2016-92, 2016
Manuscript under review for journal Hydrol. Earth Syst. Sci.
Published: 2 March 2016

Hydrology and Earth System Sciences
Discussions

682 Zreda M., Shuttleworth W. J., Xeng X., Zweck C., Desilets D., Franz T. E., Rosolem R., and
683 Ferre P. A.: COSMOS: The Cosmic-Ray Soil Moisture Observing System. *Hydrol.*
684 *Earth Syst. Sci. Discuss*., Vol. 9, Pgs. 5405-4551, doi:10.5194/ hessd-9-4505-2012, 2012.

685

686 **Table Captions**

687 Table 1. Summary of mean, standard deviation of *in-situ* lattice water samples organized by USA
688 soil taxonomic groups. The table also summarizes a linear regression analysis using the GSDE
689 clay percent and *in-situ* sample. The last column indicates how the 1 km CONUS lattice water
690 map was generated. Note NA stands for not applicable because of a lack of data.

USA Soil Taxonomic Group	Mean Lattice Water (Wt. %)	Std. Lattice Water (Wt. %)	Number of Samples	Linear Regression Slope	Linear Regression Intercept	Linear Regression R^2	Linear Regression p value	GSDE Derived CONUS Lattice Water Product
Alfisol	4.31	1.36	9	6.09	-0.11	0.086	0.44330	Mean
Andisol	NA	NA	NA	NA	NA	NA	NA	NA
Aridisol	2.73	1.36	10	4.82	-0.15	0.095	0.38607	Mean
Entisol	1.47	0.93	5	2.48	-0.14	0.233	0.41064	Mean
Gelisol	NA	NA	NA	NA	NA	NA	NA	NA
Histosol	NA	NA	NA	NA	NA	NA	NA	NA
Inceptisol	4.98	0.28	2	NA	NA	NA	NA	Mean
Mollisol	3.18	1.22	24	1.03	0.11	0.539	0.00004	Linear
Oxisol	NA	NA	NA	NA	NA	NA	NA	NA
Spodosol	2.68	2.10	4	3.45	-0.11	0.020	0.85919	Mean
Ultisol	2.82	2.33	6	0.28	0.20	0.229	0.33672	Mean
Vertisol	5.18	NA	1	NA	NA	NA	NA	NA
ALL	3.16	1.58	61	1.68	0.09	0.183	0.00066	NA

691

692

Hydrol. Earth Syst. Sci. Discuss., doi:10.5194/hess-2016-92, 2016
Manuscript under review for journal Hydrol. Earth Syst. Sci.
Published: 2 March 2016

Hydrology and Earth System Sciences
Open Access
Discussions

693 Table 2. Top) Summary of mean difference between *in-situ* samples and GSDE values (Figure 3)
694 for bulk density, lattice water and organic carbon. Bottom) Summary of covariance matrix of
695 difference between *in-situ* values and GSDE values. The mean difference and covariance data
696 were used in an error propagation analysis illustrated in Figure 6.

	Bulk Density (g/cm^3)	**Lattice Water (Wt. %)**	**Organic Carbon (Wt. %)**
Mean Difference of in-situ value - GSDE value	-0.10035	-0.05789	-0.07077
Covariance matrix of in-situ value - GSDE value			
	Bulk Density (g/cm^3)	**Lattice Water (Wt. %)**	**Organic Carbon (Wt. %)**
Bulk Density (g/cm^3)	0.0386	-0.0567	-0.2077
Lattice Water (Wt. %)		1.6745	0.3624
Organic Carbon (Wt. %)			3.5810

697

698

699 Table 3. Summary of 2014 *GrWDRVI* and calculated standing wet biomass for irrigated maize
700 and irrigated soybean fields near Waco, NE. Note that the senescence equation was applied to
701 DOY 209 for the irrigated maize field as planting date and development can vary locally. The
702 drop in *GrWDRVI* between DOY 201 and 209 is a clear indicator of change in plant growth stage
703 that can be used on a field by field basis.

DOY (2014)	**GrWDRVI, Irrigated-Maize**	**GrWDRVI-Irrigated Soybean**	**Calculated Standing Wet Biomass-Irrigated Maize (kg/m^2)**	**Calculated Standing Wet Biomass-Irrigated Soybean (kg/m^2)**
153	0.23	0.23	0.00	0.00
161	0.24	0.24	0.00	0.00
169	0.32	0.28	0.53	0.06
177	0.57	0.54	4.69	1.25

Hydrol. Earth Syst. Sci. Discuss., doi:10.5194/hess-2016-92, 2016
Manuscript under review for journal Hydrol. Earth Syst. Sci.
Published: 2 March 2016

185	0.55	NA	4.33	NA
193	0.63	0.63	5.63	1.91
201	0.61	0.71	5.34	2.48
209	0.55	0.73	6.50*	2.61
217	0.57	0.74	6.58	2.67
225	0.50	0.73	6.27	2.61
233	0.47	0.74	6.07	NA
241	0.40	0.68	5.38	2.89
249	0.43	0.64	5.73	6.77
257	0.27	0.47	1.44	6.07
265	0.25	0.44	0.00	5.83
281	0.21	0.28	0.00	2.02
289	0.21	0.26	0.00	0.78
297	0.20	0.25	0.00	0.00

704

705

706 Table 4. Summary of 2014 observed standing wet biomass for irrigated maize and irrigated
707 soybean fields near Waco, NE. The observations represent the aggregation of 18 plants collected
708 at 6 different locations across the field on the sampling date.

DOY (2014), Irrigated Soybean	**Observed Standing Wet Biomass-Irrigated Soybean (kg/m^2)**	**DOY (2014), Irrigated Maize**	**Observed Standing Wet Biomass-Irrigated Maize (kg/m^2)**
167	0.19	161	0.13
196	1.63	183	2.40
211	1.81	217	6.22
259	1.63	259	0.30

709

710

711

712

Hydrol. Earth Syst. Sci. Discuss., doi:10.5194/hess-2016-92, 2016
Manuscript under review for journal Hydrol. Earth Syst. Sci.
Published: 2 March 2016

733 **Figure Captions**

734 Figure 1. Soil taxonomic classification map over the Continental United States of America using
735 the twelve USA soil taxonomic orders (data source FAO 2007 and personal communication with
736 M. Kuzila). Note gelisols are not present in the CONUS. Black dots indicate 61 locations where
737 we have *in-situ* composite/average samples for soil bulk density, soil lattice water, soil organic
738 carbon, and clay weight fraction collected over a 12.6 ha circle and averaged over the top 30 cm
739 (Table S1).

740

741 Figure 2. Comparison between 61 *in-situ* composite sample and GSDE value from the closest
742 pixel for a) clay weight percent b) soil bulk density, and c) soil organic carbon. d) Comparison
743 between *in-situ* lattice water and derived values using GSDE clay weight fraction and soil
744 taxonomic orders. See Table 1 for summary of data by taxonomic group, Table S1 for raw data,
745 and Table 2 for statistical summary of differences between *in-situ* and GSDE product. Note error
746 bars denote +/- 1 standard deviation.

747

748 Figure 3. Derived 1 km resolution lattice water weight percent map using the GSDE clay percent
749 and regression analyses organized by soil taxonomic classification. See Table 1 for estimates of
750 the mean, standard deviation, and linear regression vs. clay percent organized by taxonomic
751 group. Black dots indicate 61 locations where we have *in-situ* composite/average samples for soil
752 bulk density, soil lattice water, soil organic carbon, and clay weight fraction collected over a 12.6
753 ha circle and averaged over the top 30 cm (Table S1). Missing areas indicate surface water
754 bodies or soil taxonomic groups with no or limited *in-situ* lattice water sampling (see Table 1).

Hydrol. Earth Syst. Sci. Discuss., doi:10.5194/hess-2016-92, 2016
Manuscript under review for journal Hydrol. Earth Syst. Sci.
Published: 2 March 2016

Hydrology and Earth System Sciences
Discussions

755

756 Figure 4. Relationship between *GrWDRVI* and observed standing weight biomass for maize (a,
757 c) and soybean (b, d) partitioned into green-up (DOY< 210 for maize, DOY<230 for soybean)
758 and senescence. Destructive vegetation data is aggregated from 3 fields near Mead, NE between
759 2003-2013 (Table S2). The regression coefficients and equations are summarized in Table S3.
760 Note that the maize and soybean functions were subject to the constraints in order to provide
761 realistic behavior at the observed *GrWDRVI* and destructive vegetation sampling bounds. See
762 main text for details.

763

764 Figure 5. Time series of standing wet biomass for two study sites (irrigated maize and irrigated
765 soybean) near Waco, NE over the 2014 growing season. The graph contains the observed *in-situ*
766 sampling in addition to the *GrWDRVI* estimates using the equations summarized in Table S3.
767 See Table 3 for *GrWDRVI* values and Table 4 for *in-situ* estimates.

768

769 Figure 6. Propagation of error analysis using Monte Carlo simulations of 100,000 soil parameter
770 datasets of true soil parameters (i.e. soil bulk density, lattice water, soil organic carbon) and
771 perturbed parameters with matching mean differences and covariance matrix between *in-situ*
772 samples and GSDE derived parameters (see Table 2). Three error metrics are presented across a
773 range of neutron counts (and thus *SWC* values). Note that soil bulk density was constrained to
774 1.2-1.5 g/cm^3, lattice water was constrained from 1-8 wt. %, soil organic carbon was constrained
775 from 0-8 wt. %, and soil water content was constrained from 0.03-0.45 cm^3/cm^3. Simulated and
776 calculated values outside of these bounds were either reset to the minimum or maximum or

Hydrol. Earth Syst. Sci. Discuss., doi:10.5194/hess-2016-92, 2016
Manuscript under review for journal Hydrol. Earth Syst. Sci.
Published: 2 March 2016

777 removed from the Monte Carlo statistics. A minimum threshold of 70% of simulated cases were

778 used to compute error statistics.

Hydrol. Earth Syst. Sci. Discuss., doi:10.5194/hess-2016-92, 2016
Manuscript under review for journal Hydrol. Earth Syst. Sci.
Published: 2 March 2016

Hydrology and Earth System Sciences
Discussions

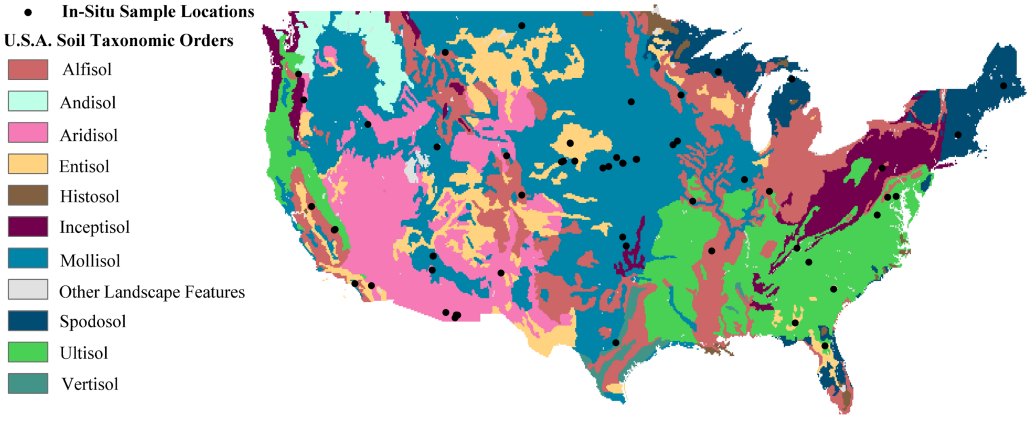

Figure 1. Soil taxonomic classification map over the Continental United States of America using the twelve USA soil taxonomic orders (data source FAO 2007 and personal communication with M. Kuzila). Note gelisols are not present in the CONUS. Black dots indicate 61 locations where we have *in-situ* composite/average samples for soil bulk density, soil lattice water, soil organic carbon, and clay weight fraction collected over a 12.6 ha circle and averaged over the top 30 cm (Table S1).

Hydrol. Earth Syst. Sci. Discuss., doi:10.5194/hess-2016-92, 2016
Manuscript under review for journal Hydrol. Earth Syst. Sci.
Published: 2 March 2016

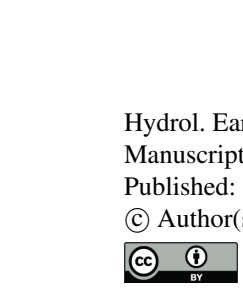

Hydrology and Earth System Sciences
Discussions

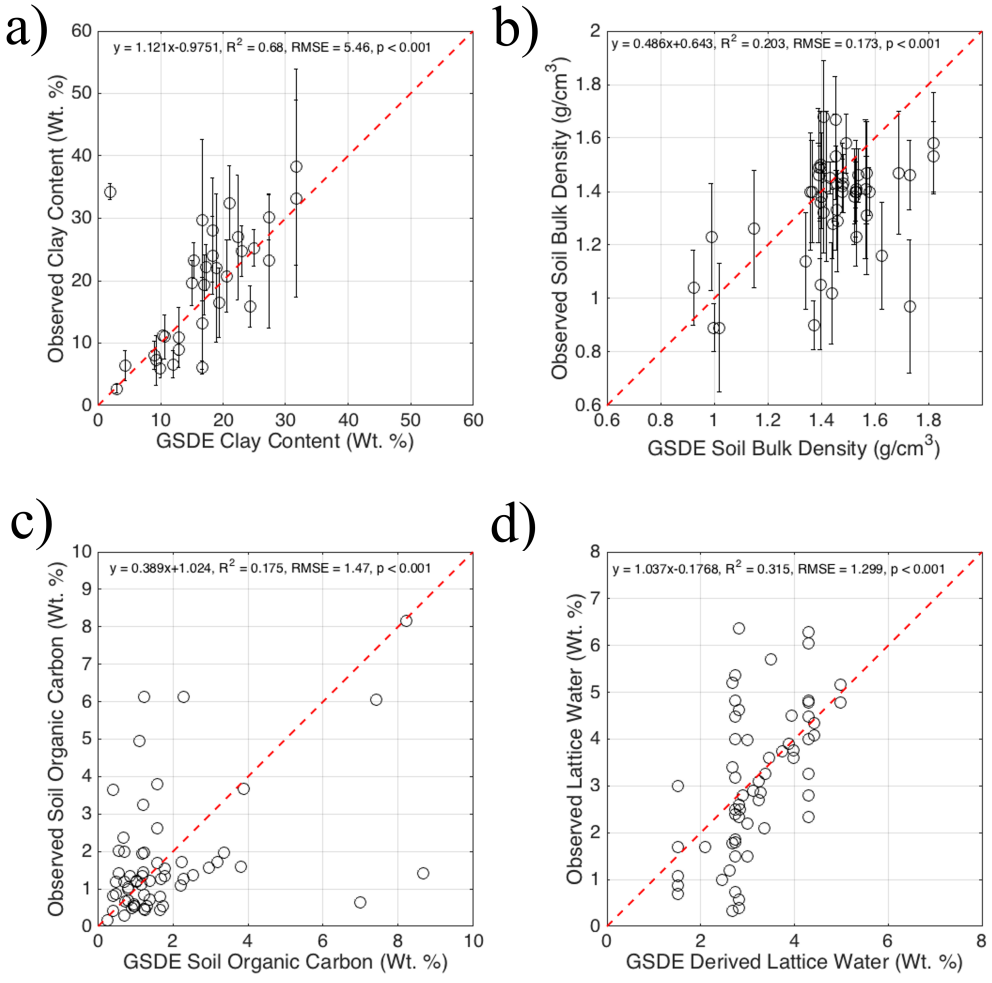

Figure 2. Comparison between 61 *in-situ* composite sample and GSDE value from the closest pixel for a) clay weight percent b) soil bulk density, and c) soil organic carbon. d) Comparison between *in-situ* lattice water and derived values using GSDE clay weight fraction and soil taxonomic orders. See Table 1 for summary of data by taxonomic group, Table S1 for raw data, and Table 2 for statistical summary of differences between *in-situ* and GSDE product. Note error bars denote +/- 1 standard deviation.

Hydrol. Earth Syst. Sci. Discuss., doi:10.5194/hess-2016-92, 2016
Manuscript under review for journal Hydrol. Earth Syst. Sci.
Published: 2 March 2016

Hydrology and Earth System Sciences
Discussions

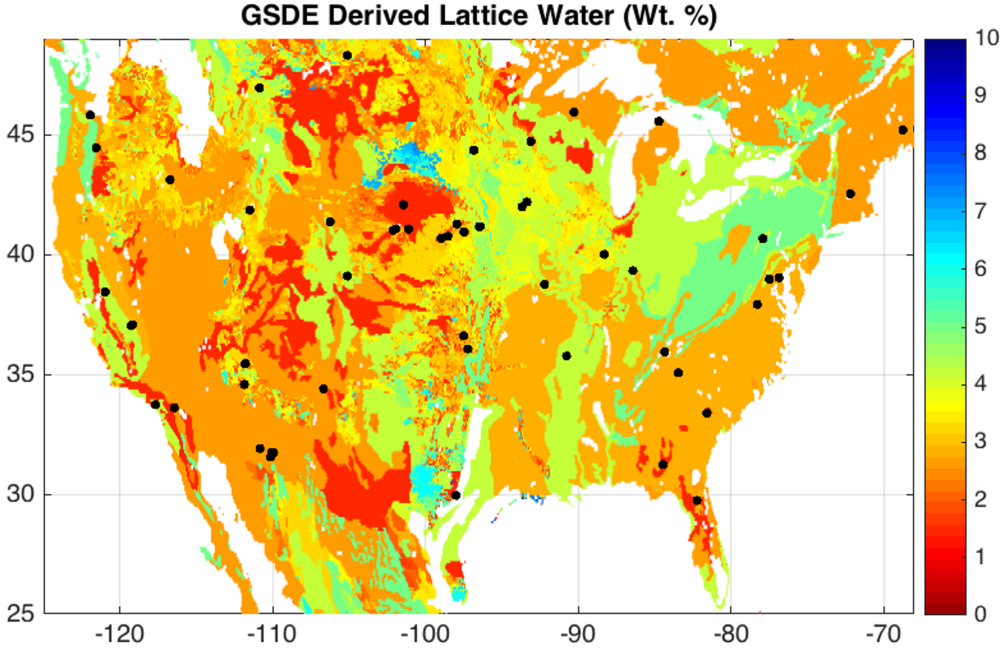

Figure 3. Derived 1 km resolution lattice water weight percent map using the GSDE clay percent and regression analyses organized by soil taxonomic classification. See Table 1 for estimates of the mean, standard deviation, and linear regression vs. clay percent organized by taxonomic group. Black dots indicate 61 locations where we have *in-situ* composite/average samples for soil bulk density, soil lattice water, soil organic carbon, and clay weight fraction collected over a 12.6 ha circle and averaged over the top 30 cm (Table S1). Missing areas indicate surface water bodies or soil taxonomic groups with no or limited *in-situ* lattice water sampling (see Table 1).

Hydrol. Earth Syst. Sci. Discuss., doi:10.5194/hess-2016-92, 2016
Manuscript under review for journal Hydrol. Earth Syst. Sci.
Published: 2 March 2016

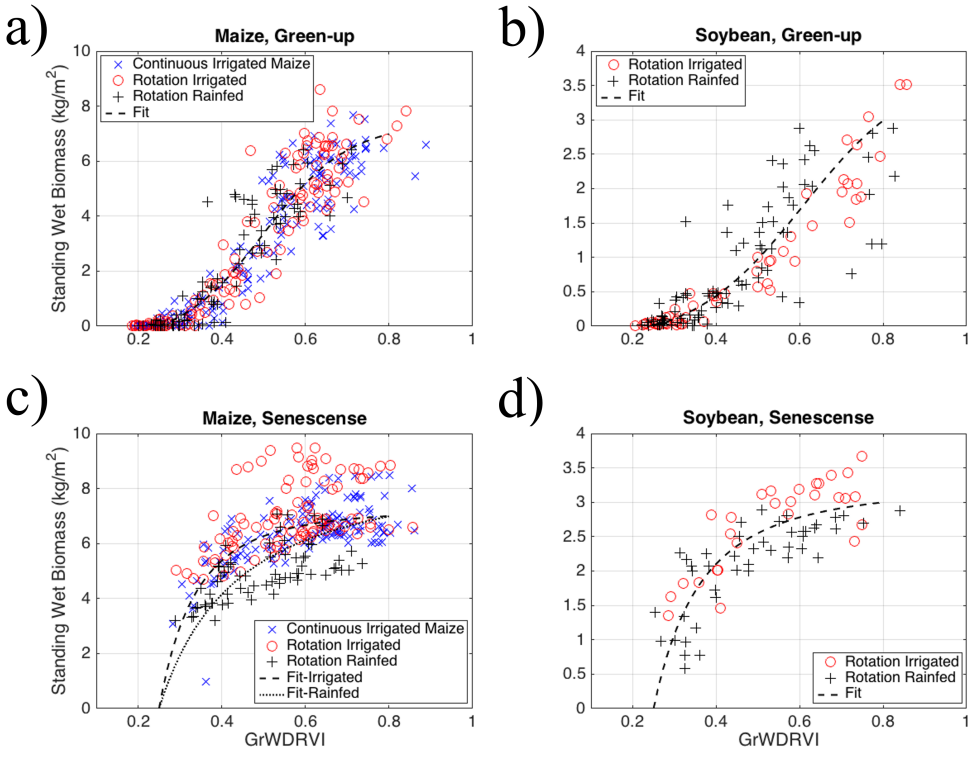

Figure 4. Relationship between *GrWDRVI* and observed standing weight biomass for maize (a, c) and soybean (b, d) partitioned into green-up (DOY<210 for maize, DOY<230 for soybean) and senescence. Destructive vegetation data is aggregated from 3 fields near Mead, NE between 2003-2013 (Table S2). The regression coefficients and equations are summarized in Table S3. Note that the maize and soybean functions were subject to the constraints in order to provide realistic behavior at the observed *GrWDRVI* and destructive vegetation sampling bounds. See main text for details.

Hydrol. Earth Syst. Sci. Discuss., doi:10.5194/hess-2016-92, 2016
Manuscript under review for journal Hydrol. Earth Syst. Sci.
Published: 2 March 2016

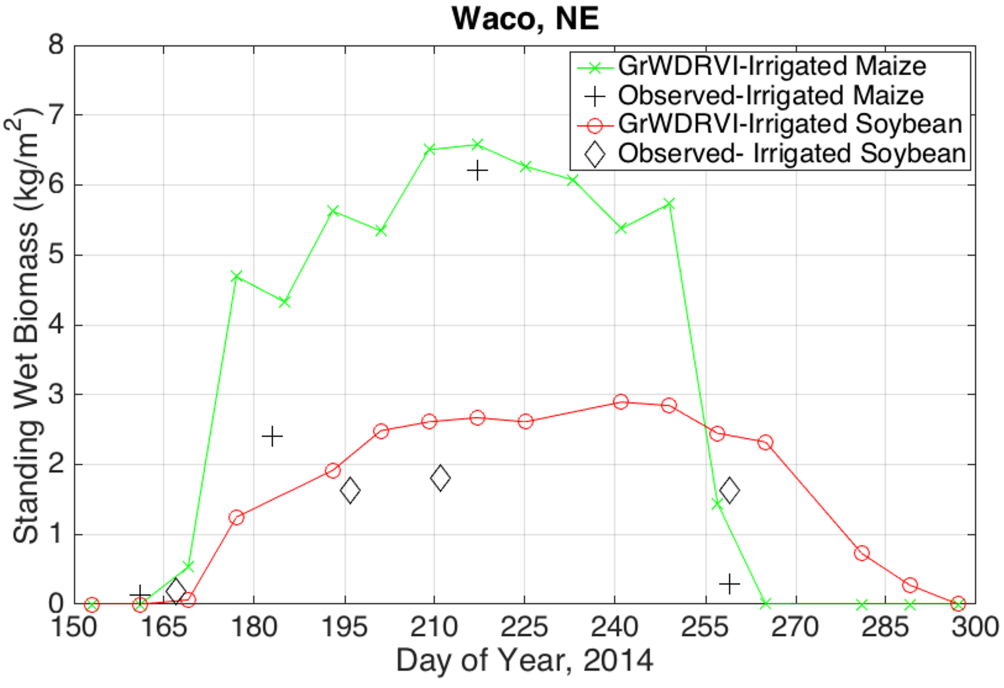

Figure 5. Time series of standing wet biomass for two study sites (irrigated maize and irrigated soybean) near Waco, NE over the 2014 growing season. The graph contains the observed *in-situ* sampling in addition to the *GrWDRVI* estimates using the equations summarized in Table S3. See Table 3 for *GrWDRVI* values and Table 4 for *in-situ* estimates.

Hydrol. Earth Syst. Sci. Discuss., doi:10.5194/hess-2016-92, 2016
Manuscript under review for journal Hydrol. Earth Syst. Sci.
Published: 2 March 2016

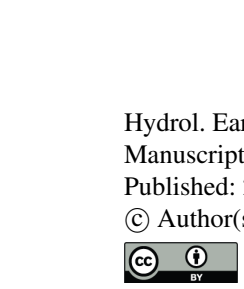

Hydrology and Earth System Sciences
Discussions

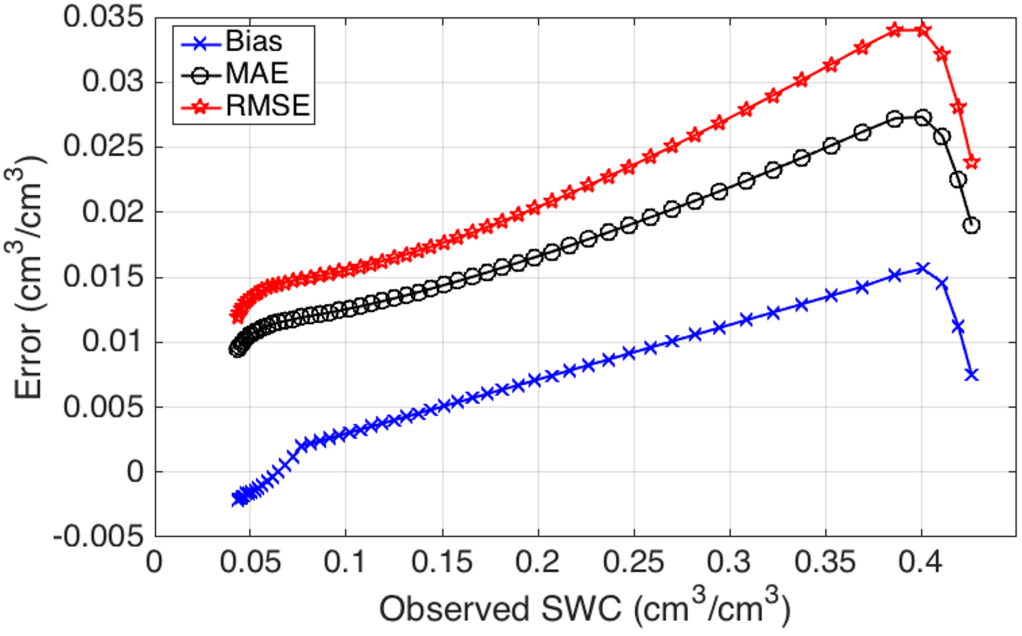

Figure 6. Propagation of error analysis using Monte Carlo simulations of 100,000 soil parameter datasets of true soil parameters (i.e. soil bulk density, lattice water, soil organic carbon) and perturbed parameters with matching mean differences and covariance matrix between *in-situ* samples and GSDE derived parameters (see Table 2). Three error metrics are presented across a range of neutron counts (and thus *SWC* values). Note that soil bulk density was constrained to 1.2-1.5 g/cm^3, lattice water was constrained from 1-8 wt. %, soil organic carbon was constrained from 0-8 wt. %, and soil water content was constrained from 0.03-0.45 cm^3/cm^3. Simulated and calculated values outside of these bounds were either reset to the minimum or maximum or removed from the Monte Carlo statistics. A minimum threshold of 70% of simulated cases were used to compute error statistics.